EC
Journals.ASM.org

Identification of Obscure yet Conserved Actin-Associated Proteins in *Giardia lamblia*

Alexander R. Paredez,[a,b] Arash Nayeri,[b] Jennifer W. Xu,[a,b] Jana Krtková,[a] W. Zacheus Cande[b]

Department of Biology, University of Washington, Seattle, Washington, USA[a]; Department of Molecular and Cell Biology, University of California at Berkeley, Berkeley, California, USA[b]

Consistent with its proposed status as an early branching eukaryote, *Giardia* has the most divergent actin of any eukaryote and lacks core actin regulators. Although conserved actin-binding proteins are missing from *Giardia*, its actin is utilized similarly to that of other eukaryotes and functions in core cellular processes such as cellular organization, endocytosis, and cytokinesis. We set out to identify actin-binding proteins in *Giardia* using affinity purification coupled with mass spectroscopy (multidimensional protein identification technology [MudPIT]) and have identified >80 putative actin-binding proteins. Several of these have homology to conserved proteins known to complex with actin for functions in the nucleus and flagella. We validated localization and interaction for seven of these proteins, including 14-3-3, a known cytoskeletal regulator with a controversial relationship to actin. Our results indicate that although *Giardia* lacks canonical actin-binding proteins, there is a conserved set of actin-interacting proteins that are evolutionarily indispensable and perhaps represent some of the earliest functions of the actin cytoskeleton.

In addition to being a major parasite infecting more than 280 million people each year, *Giardia lamblia* (synonymous with *Giardia intestinalis* and *Giardia duodenalis*) belongs to one of the earliest diverging groups of eukaryotes (1–4). Therefore, investigation of *Giardia* biology has the potential to uncover evolutionarily deep cellular mechanisms. However, the placement of *Giardia* near the root of the eukaryotic tree, in addition to the placement of the root itself, is contentious (5). Nevertheless, *Giardia* is the most divergent eukaryote that can be manipulated in the laboratory with molecular and genetic tools (4, 6–10). In addition, many pathways in *Giardia* have fewer components than in the well-studied model eukaryotes (4). Thus, the combination of *Giardia*'s highly divergent and minimalistic genome provides a unique perspective through which cellular processes may be examined. This perspective may potentially define both the minimal requirements for function and the portions of cellular mechanisms constrained throughout evolution.

A major point of divergence between *Giardia* and other eukaryotes is the cytoskeleton (11). *Giardia* lacks the canonical actin-binding proteins, once thought common to all extant eukaryotes, which perform critical functions in other eukaryotes (12). Their absence may indicate a split from the last eukaryotic common ancestor before the canonical set of actin-binding proteins was established. Alternatively, *Giardia* may have evolved a novel set of actin-interacting proteins that allowed for the gradual loss of the canonical set of actin-binding proteins (11, 13). Our previous work has shown that despite the lack of canonical actin-binding proteins, *Giardia* actin (giActin) is required for conserved cellular functions, including membrane trafficking, cytokinesis, polarity, and control of cellular morphology (13). The *Giardia* cytoskeleton is also quite elaborate, suggesting the presence of cytoskeletal regulators (Fig. 1). That giActin performs similar functions to actin in other eukaryotes suggests these processes were already associated with actin at the time *Giardia* split from the other eukaryotes (13). We have also shown that giRac, the sole Rho family GTPase in *Giardia*, regulates actin despite the absence of all actin-binding proteins known to link G-protein signaling to the actin cytoskeleton (Arp2/3, formin, wave, myosin, and cofilin) (13). Therefore, *Giardia* must contain a novel set of actin-interacting proteins comprised of ancient yet undiscovered and/or *Giardia*-specific actin regulators. We sought here to identify actin-binding proteins using actin affinity chromatography coupled with multidimensional protein identification technology (MudPIT) (14). The discovery of *Giardia*-specific actin-binding proteins with essential functions would open an avenue to potential therapeutic targets, while the discovery of conserved proteins would highlight an ancient relationship between actin and the identified protein, worthy of further exploration.

MATERIALS AND METHODS

Strain and culture conditions. *Giardia lamblia*, strain WBC6 was cultured as described previously (15). Morpholino knockdown experiments and quantitative Western blotting were performed as described previously (9, 13). Large volume high-yield cultures required a method to increase the surface area. We filled standard wide-mouth media bottles with cut-to-length "jumbo drinking straws" and autoclaved them before filling with media (see Fig. S1 in the supplemental material). *Giardia* cell counts increased by ~30% in straw-filled 500-ml bottles versus those without. After 3 days of growth, we did not observe unattached cells at the bottom of straw-filled culture vessels that are typical of overgrown cultures, while bottles without straws had a layer of cell sediment. After 72 h of growth 1-liter cultures regularly reach 2.5×10^6 cells/ml, exceeding maximum trophozoite concentrations obtained with Farthing's roller bottles, without needing specialized equipment (16).

Received 13 February 2014 Accepted 5 April 2014
Published ahead of print 11 April 2014
Address correspondence to Alexander R. Paredez, aparedez@uw.edu.
Supplemental material for this article may be found at http://dx.doi.org/10.1128/EC.00041-14.

doi:10.1128/EC.00041-14

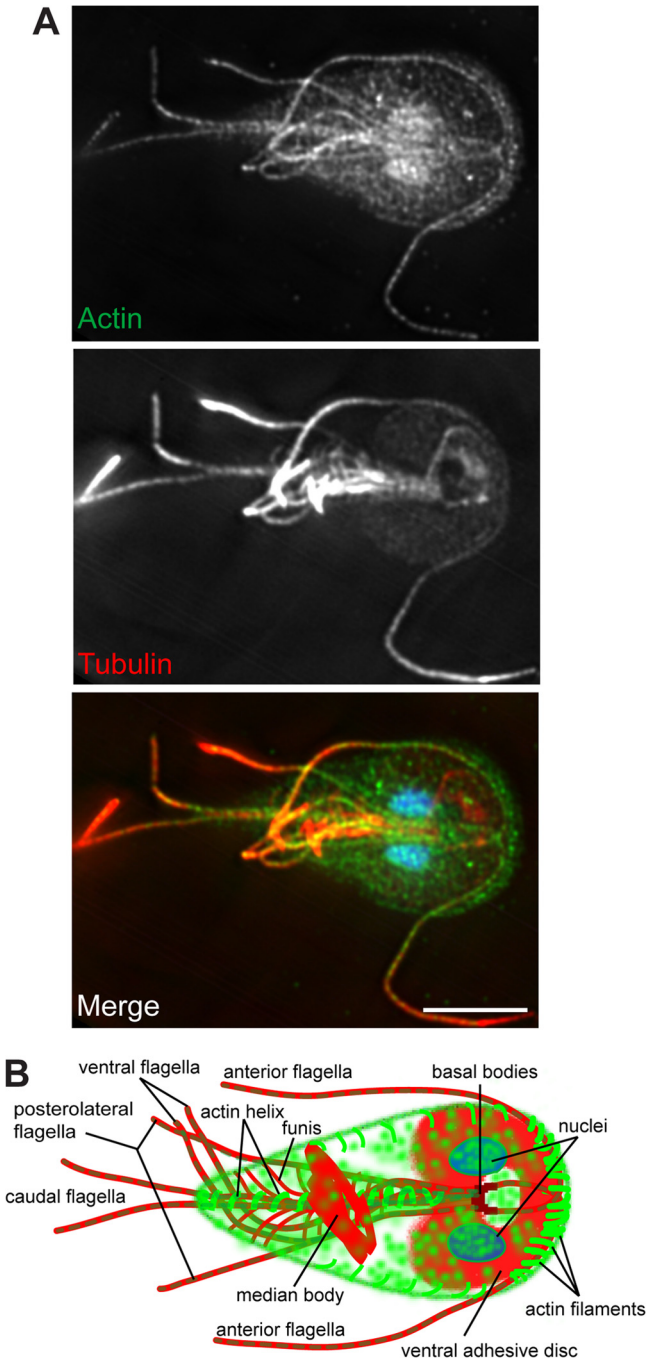

FIG 1 *Giardia* cytoskeletal organization. (A) Maximum projection of a Z-stack. Actin is green, tubulin is red, and DNA is blue. (B) Diagram of *Giardia* trophozoite with all of the prominent cytoskeletal structures labeled.

Constructs. The TS-Actin vector was constructed by modifying pGFPapac (17). A BamHI site was first introduced between BsrGI and NotI of enhanced green fluorescent protein (eGFP) using an oligonucleotide adapter; all primer sequences can be found in Table S1 in the supplemental material. The glutamate dehydrogenase (GDH) promoter was exchanged for the actin promoter by excising GDH with HindIII and NcoI, the actin promoter was subsequently ligated into the same position. Next. eGFP was excised with NcoI and BamHI, allowing for the TwinStrep tag to be ligated into the same position. Finally, the vector was digested with BamHI and NotI so that the actin gene could be ligated into the vector. All PCR amplification steps were performed with iProof high-fidelity polymerase (Bio-Rad), and the resulting vectors were verified by sequencing. The putative actin-interacting proteins were PCR amplified from genomic DNA and inserted into the pKS 3HA.NEO vector (10) using the restriction sites indicated in Table S1 in the supplemental material. All resulting constructs except for TS-Actin, GL50803_6744, and GL50803_13273 were linearized and integrated into the genome by homologous recombination to generate endogenously tagged proteins.

Actin affinity chromatography. One-liter straw-packed and sterilized bottles were filled with medium and inoculated with two 13-ml confluent cultures containing wild-type (WT) or TwinStrep-giActin cell lines. After 3 days the cultures were incubated in an ice water bath for 1 h to detach cells. The media and unattached cells were transferred to centrifuge bottles and pelleted at 750 × *g* for 15 min. The resulting cell pellet was washed in 10 ml of cold HEPES-buffered saline, transferred to 15-ml conical tubes, and pelleted again. The cell pellet was resuspended in an equal volume (~2 ml) of lysis buffer (50 mM Tris, pH 7.5, 150 mM NaCl, 7.5% glycerol, 0.25 mM $CaCl_2$, 0.25 mM ATP, 0.05 mM dithiothreitol [DTT], 0.5 mM phenylmethylsulfonyl fluoride [PMSF], 2× Halt protease inhibitors [Pierce]). The pellet was stored overnight at −80°C and, after thawing, the cells were sonicated, and the extract cleared at 10,000 × *g* for 10 min. The lysate was added to 200 μl of Streptactin-Sepharose beads (IBA) previously equilibrated with lysis buffer. Binding was performed for 1.5 h with end-over-end mixing at 4°C. The beads were washed once in batch (100 mM Tris, pH 8.0, 150 mM NaCl, 7.5% glycerol, 0.25 mM $CaCl_2$, 0.25 mM ATP, 0.5 mM DTT) and then moved into a chromatography column (Bio-Rad) and washed four additional times with one column bed volume of wash buffer. Protein was eluted with 6 half-column bed volumes with elution buffer (100 mM Tris, pH 8.0, 150 mM NaCl, 7.5% glycerol, 0.25 mM $CaCl_2$, 0.25 mM ATP, 0.5 mM DTT, 2 mM D-biotin).

Actin pelleting assay. TwinStrep-Actin was purified as described above and then dialyzed for 2 h in G buffer (5 mM Tris, pH 8.0, 0.2 mM ATP, 0.2 mM $CaCl_2$, 0.5 mM dithiothreitol). After a buffer exchange, the actin was dialyzed overnight. The dialyzed actin was cleared by centrifugation at 100,000 × *g* for 30 min to remove aggregates. A 1/10 volume of 10× KMEI80 (800 mM KCl, 10 mM $MgCl_2$, 10 mM EGTA, 100 mM imidazole [pH 7.0]) was added to the cleared actin, followed by incubation for 30 min at room temperature. The KMEI80-actin mixture was then centrifuged at 100,000 × *g* for 30 min.

Mass spectroscopy. Mass spectrometry was performed by the Vincent J. Coates Proteomics/Mass Spectrometry Laboratory at UC Berkeley. The protein solution was adjusted to 8 M urea, subjected to carboxyamidomethylation of cysteines, and digested with trypsin. The sample was then desalted using a c18 spec tip (Varian). A nano-LC column was packed in a 100-μm-inner-diameter glass capillary with an emitter tip. The column consisted of 10 cm of Polaris c18 5-μm packing material (Varian), followed by 4 cm of Partisphere 5 SCX (Whatman). The column was loaded by using a pressure bomb and washed extensively with buffer A (see below). The column was then directly coupled to an electrospray ionization source mounted on a Thermo-Fisher LTQ XL linear ion trap mass spectrometer. An Agilent 1200 high-pressure liquid chromatograph equipped with a split line so as to deliver a flow rate of 300 nl/min was used for chromatography. Peptides were eluted using an eight-step MudPIT procedure (14). Buffer A was 5% acetonitrile–0.02% heptafluorobutyric acid (HBFA); buffer B was 80% acetonitrile–0.02% HBFA. Buffer C was 250 mM ammonium acetate–5% acetonitrile–0.02% HBFA; buffer D was the same as buffer C, but with 500 mM ammonium acetate. The programs SEQUEST and DTASelect were used to identify peptides and proteins from the *Giardia* database (18, 19).

Immunoprecipitation and Western blotting. Immunoprecipitation began with a single confluent 13-ml tube per cell line. After detachment, cells were pelleted at 900 × *g* and washed once in HBS. The cells were resuspended in 300 μl of lysis buffer (50 mM Tris 7.5, 150 mM NaCl, 7.5% glycerol, 0.25 mM $CaCl_2$, 0.25 mM ATP, 0.5 mM DTT, 0.5 mM PMSF,

0.1% Triton X-100, 2× Halt protease inhibitors [Pierce]) and sonicated. The lysate was cleared by centrifugation at 10,000 × *g* for 10 min at 4°C and then added to 30 μl of anti-HA beads (Sigma). After 1.5 h of binding, the beads were washed four times with wash buffer (25 mM Tris 7.5, 150 mM NaCl, 0.25 mM $CaCl_2$, 0.25 mM ATP, 5% glycerol, 0.05% Tween 20) and then boiled in 50 μl of sample buffer. Western blotting was performed as described previously (13). Rabbit anti-giActin polyclonal (13) and anti-HA mouse monoclonal HA7 antibody (Sigma-Aldrich) were both used at 1:3,000. Fluorescent secondary antibodies (Li-Cor) were used at 1:15,000, horseradish peroxidase-linked anti-rabbit antibodies (Bio-Rad) were used at 1:7,000.

Microscopy. Fixations were performed as described previously (13). Anti-HA mouse monoclonal HA7 antibody (Sigma-Aldrich) was used at 1:125, and anti-mouse and anti-rabbit secondary antibodies were used at 1:200 (Molecular Probes). Images were acquired on a DeltaVision Elite microscope using a 100× 1.4 NA objective and a CoolSnap HQ2 camera. Deconvolution was performed with SoftWorx (API, Issaquah, WA). Maximal projections were made with ImageJ (20), and figures were assembled using the Adobe Creative Suite (Mountain View, CA).

RESULTS

We set out to identify giActin interactors via an affinity chromatography approach utilizing the TwinStrep Tag (21–23). Actin is notoriously sensitive to chimeric fusions, because epitope or fluorescent protein fusions may cause steric interference or otherwise affect filament formation and dynamics (24). Thus, we devised a strategy to test whether our TwinStrep-Actin fusion (TS-Actin) was functional *in vivo*. Previous work demonstrated that actin can be effectively depleted with translation-blocking morpholinos (13). These antisense morpholinos bind to the start of the transcript and block translation initiation machinery from recognizing the start codon (9, 13). Therefore, by fusing TwinStrep to the N terminus of giActin, we generated a morpholino-insensitive version of giActin. In this case, morpholino treatment is expected to block translation of endogenous actin, whereas it should have no effect on the transgenic version. We also sought to maintain actin levels near endogenous levels by driving expression of our TS-Actin fusion with the native actin promoter.

Quantitative Western blotting with an anti-giActin polyclonal antibody (13) indicated that although we used the native promoter, there was roughly a 4-fold increase in total actin levels compared to nontransgenic controls; ca. 75% of this was TS-Actin (Fig. 2A). The higher levels of transgenic actin are presumably due to the copy number of our episomally maintained construct exceeding the number of endogenous actin genes. Morpholino treatment of the TS-Actin-expressing cell line behaved as predicted; the N-terminal epitope tag protected TS-Actin from being depleted by anti-actin morpholinos, while the endogenous actin was depleted to ~20% of control levels (Fig. 2A). Further, we examined the morpholino-treated cells for morphological defects associated with actin depletion such as abnormal cell shape, out-of-position flagella, and multiple or out-of-position nuclei (13). In the control-treated cell line we observed a slight increase in the number of abnormal cells: 6.6% for TS-Actin ($n = 600$) versus 1.9% for wild-type ($n = 400$), indicating that the increased actin levels and/or the epitope tag mildly interfered with normal actin function (Fig. 2B). The transgenic line was, however, resistant to morpholino depletion since the proportion of abnormal cells remained at 6.8% ($n = 600$) after morpholino treatment. In contrast, 35.2% of the WT cells ($n = 500$) treated with the anti-actin morpholinos had abnormal morphology. Therefore, we conclude

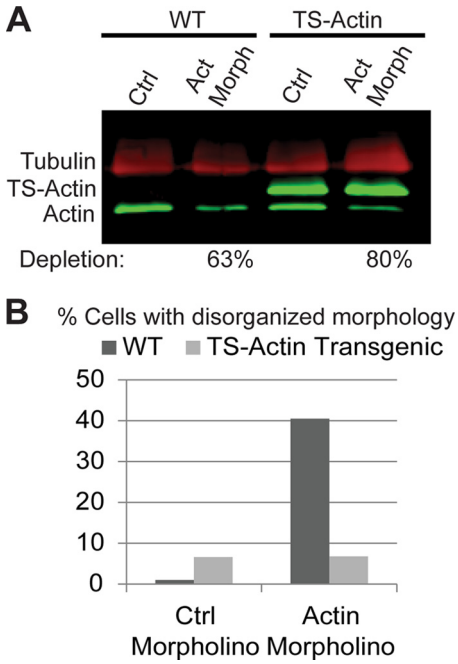

FIG 2 TS-Actin is functional *in vivo*. (A) Multiplex Western blot (actin, green; tubulin, red) showing that TS-Actin is morpholino resistant, while endogenous actin is significantly reduced. (B) Reducing endogenous actin results in cellular disorganization, morpholino-resistant TS-Actin can substitute for endogenous actin.

that TS-Actin can partially rescue endogenous actin depletion, indicating that TS-Actin is functional *in vivo*.

A particular challenge of producing large-scale *Giardia* cultures, sufficient for biochemical analysis, is the need to provide surface area for adherent growth. *Giardia* is an extracellular parasite that colonizes the host intestine by attaching via its "suction cup" organelle, the ventral disc (25, 26). Likewise, in the laboratory *Giardia* trophozoites grow attached to the sides of the culture tubes. Cultures cease to proliferate after the culture tubes are confluent with cells. Free-floating cells are often observed to have an aberrant morphology, indicating the importance of surface attachment, possibly because *Giardia* divides by an adhesion-dependent mechanism (27, 28). Custom "inside-out" roller bottles have been used by others to grow high-yield *Giardia* cultures, but these are not commercially available (16). We developed a low-cost high-yield method of growing *Giardia* by inserting common polypropylene drinking straws into wide mouth bottles (see Fig. S1 in the supplemental material and see Materials and Methods). Using our high-surface-area culture system, 1-liter cultures of WT and the TS-Actin transgenic cell lines produced ~2-ml cell pellets. Extracts from these cell pellets were affinity purified in parallel. The elutions from a pilot experiment were concentrated before sodium dodecyl sulfate (SDS) analysis so that ~50% of the eluted protein could be analyzed by SDS-PAGE. Many unique bands are apparent in the TS-Actin sample (Fig. 3A). The purification was repeated for mass spectroscopy analysis; Fig. 3B represents 5% of the elutions that were analyzed by mass spectroscopy. Table 1 lists 57 proteins that were unique to the TS-Actin sample and had a minimum of five detected peptides. The complete list, including low-abundance hits and proteins also identified in our mock control, is given in Table S2 in the supplemental material. Bioinfor-

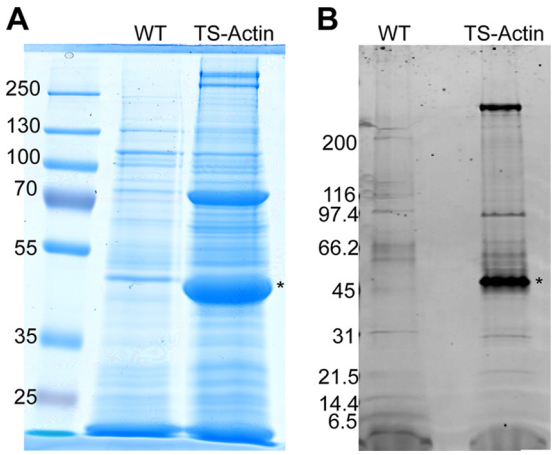

FIG 3 Isolation of TS-Actin and interacting proteins. (A) Elutions from streptactin columns for both WT and TS-Actin purifications were concentrated and then analyzed by SDS-PAGE. Note that several bands are unique to the TS-Actin cell line. Actin is marked with an asterisk. (B) Five percent of the TS-Actin purification used in the MudPIT analysis was loaded onto a 4 to 16% gradient gel and stained with SYPRO Ruby.

matics analysis was utilized to place these hits into six categories (Table 1; see Table S2 in the supplemental material).

We identified several hits that support the quality and relevance of this data set. For example, we identified all eight subunits of the TCP-1 chaperonin complex, which has an important role in folding actin (29). In addition, two proteins, p28 dynein light chain (p28 DLC) and centrin, were found in the giActin interactome, which we had previously hypothesized to be conserved actin-interacting proteins (13). Genetic and biochemical analysis of flagellar components has demonstrated that actin has an important role in flagella, where it functions in the inner dynein arm complexes (30–32). Within the inner dynein arms, p28 DLC and centrin, have been demonstrated to directly interact with actin (32). In *Giardia*, actin is readily detectable within all eight flagella, and both p28 DLC and centrin are conserved (13). In terms of peptides per molecular weight, p28 DLC was the most abundant interactor identified in our analysis. In addition to these examples, homologs of several other proteins that have been reported to complex with actin in other eukaryotes were identified and are indicated in Table 1.

The genome of *Spironucleus salmonicida*, another diplomonad and close relative of *Giardia*, was recently released (33). As part of our analysis, we compared our list of putative actin interactors to the *S. salmonicida* genome (Table 1) (33). Although most of the identified proteins are present in *S. salmonicida*, several appear to be specific to *Giardia*. We also searched the *S. salmonicida* genome for the presence of canonical actin-binding proteins. Intriguingly, we found that *S. salmonicida* contains several actin-binding proteins not found in *Giardia*; these include formin, cofilin, and coronin (see Table S3 in the supplemental material). *S. salmonicida*, however, lacks many canonical actin-binding proteins, including the Arp2/3 complex, nucleation-promoting factors, dynactin, capping protein, and myosin. Nevertheless, the subset of canonical actin-binding proteins in *S. salmonicida* suggests the loss of such proteins from *Giardia*. Without additional genomes, we can only speculate whether the diplomonads ever had the full complement of actin-binding proteins; however, the absence of myosin in *Giardia*, *S. salmonicida*, and *Trichomonas vaginalis* (a nondiplimonad excavate) remains consistent with the idea that a subset of excavates may have split from the other eukaryotes before the full complement of actin-binding proteins was established (4, 34). This possibility could help explain how *Giardia* could have lost proteins that are essential in the model eukaryotes.

Next, we sought to validate a subset of the conserved interactions through reciprocal immunoprecipitations. We selected nine representative proteins, at least one from each of the conserved categories; these are indicated by an asterisk in Table 1. In each case, we tagged the identified protein with a C-terminal triple HA tag. We were able to verify complex formation with giActin for p28 DLC, centrin, HSP70, ARP7, TIP49, ERK2, and 14-3-3 (Fig. 4A). Attempts to validate dynamin (Fig. 4A) and myeloid leukemia factor (MLF; data not shown) were unsuccessful. Both dynamin and MLF have been shown to interact with actin and alter filament organization in other eukaryotes (35, 36). Although these hits may be false positives, it is also possible that the C-terminal tag disrupted interaction or that the lower concentration of cell extracts in our immunoprecipitation experiments versus large-scale affinity chromatography failed to maintain integrity of the complex.

To better understand the relationship between these conserved interactors and actin, we colocalized actin and the tagged interactors (Fig. 4B). Each protein displayed a localization pattern consistent with its proposed function. p28 DLC localized to flagella. Centrin localized to the basal bodies and around a portion of the internal axonemes of the posterolateral flagella. ARP7, TIP49, and ERK2 localized to the nuclei with various amounts of non-nuclear localization. HSP70 and 14-3-3 were found throughout the cell with slight enrichment at the cell anterior. None of these conserved proteins colocalized with prominent filamentous actin structures (see Fig. 1), which is consistent with the idea that they complex with G-actin (discussed below). It should be noted that standard tools such as fluorescent phalloidin and DNase I typically used to distinguish between monomeric and filamentous actin do not work in *Giardia* (13).

DISCUSSION

In this study, we undertook a biochemical approach to identify actin interactors in *Giardia*. Our easily adopted method for growing large-scale cultures and the use of the TwinStrep tag have the potential to make the process of defining interactomes routine in *Giardia*. During the course of our study, Svard and coworkers published a TAP-tagging approach for proteomics in *Giardia* (37). Similar to our approach, these researchers used two tandem Strep II tags but also included a Flag tag, the entirety of which is known as the SF-TAP tag. They overcame the surface area issues by distributing 2 liters of medium among 40 50-ml conical tubes. Our straw method simplifies cell culture, and our ability to identify actin-interacting proteins in a single purification step suggests that tandem purification is not generally required. This is significant because single-step purifications are able to isolate weaker interactors commonly lost in two-step purifications (22). Indeed, our laboratories have already performed proteomic analysis on two additional proteins using this approach. In all cases, 1 liter of medium was sufficient for isolating protein-protein interactors. Although analysis is still under way, in each case a unique set of high-frequency hits were identified. Conversely, several low-frequency hits are common to our data sets. One data set is for Polo-

TABLE 1 Identified interactors

Protein identification no.[a]	Name and/or description	Mol wt	No. of peptides	Interactor[b]	Reference(s)	*S. salmonicida* GenBank no.[c]
Axonemal/cytoskeleton						
GL50803_111950	Axonemal dynein heavy chain	570,319	900	Precedents	32, 39	EST41976, 0.0
GL50803_101138	Axonemal dynein heavy chain	578,219	849	Precedents	32, 39	EST46166.1, 0.0
GL50803_40496	Axonemal dynein heavy chain	553,424	778	Precedents	32, 39	EST44588.1, 0.0
GL50803_13273*	P28 axonemal dynein light chain	26,895	294	IP+++	32, 39	EST43975.1, 6E–138
GL50803_42285	Axonemal dynein heavy chain 11	834,759	48	Precedents	32, 39	EST41750.1, 2E–61
GL50803_6744*	Centrin	18,687	46	IP+	32, 39	EST41812.1, 2E–98
GL50803_37985	Dynein heavy chain	118,679	26	Precedents	32, 39	EST48250.1, 0.0
GL50803_137716	Axoneme-associated protein GASP-180	174,782	24			No
GL50803_16424*	Myeloid leukemia factor like	29,702	14	IP−	35	EST47319.1, 9E–17
GL50803_14242	Dynein heavy chain-cytoplasmic	633,335	11			EST46283.1, 1E–27
Chaperone						
GL50803_11992	TCP-1 chaperonin subunit epsilon	61,193	223	Precedents	29	EST46493.1, 0.0
GL50803_11397	TCP-1 chaperonin subunit beta	56,604	204	Precedents	29	EST41446.1, 0.0
GL50803_16124	TCP-1 chaperonin subunit eta	64,752	196	Precedents	29	EST48572.1, 0.0
GL50803_13500	TCP-1 chaperonin subunit theta	60,646	187	Precedents	29	EST46649.1, 0.0
GL50803_10231	TCP-1 chaperonin subunit zeta	60,941	118	Precedents	29	EST48976.1, 0.0
GL50803_17482	TCP-1 chaperonin subunit delta	56,324	86	Precedents	29	EST41630.1, 4E–173
GL50803_91919	TCP-1 chaperonin subunit alpha	59,281	82	Precedents	29	EST47029.1, 0.0
GL50803_17411	TCP-1 chaperonin subunit gamma	61,559	71	Precedents	29	EST41533.1, 0.0
GL50803_88765*	Cytosolic HSP70	71,633	22	IP+	52	EST45839, 0.0
GL50803_17121	Bip	74,360	12		53	EST46254.1, 0.0
Nuclear						
GL50803_9825*	TBP-interacting protein TIP49	51,418	276	IP+++	54–56	EST49365.1, 0.0
GL50803_17565	TBP-interacting protein TIP49	52,616	162	Precedents	54–56	EST48144.1, 0.0
GL50803_15113*	ARP7-like	51,465	90	IP+	54–56	EST44310.1, 6E–31
GL50803_9705	Hypothetical/YEATS domain	30,449	23			EST47502.1, 1E–27
GL50803_8125	SMARCC1	47,004	17	Precedents	54–56	No
GL50803_2851	Histone acetyltransferase MYST2	49,916	12	Precedents	54–56	EST45122.1, 9E–78
GL50803_6886	Prokaryotic SMC domain protein	102,836	11			No
GL50803_17461	SWIRM domain protein	124,241	7			EST47570.1, 3E–51
Signaling						
GL50803_6317	Putative DUB	150,389	16			EST43894.1,1E–14
GL50803_22850*	ERK7-like/giERK2	41,096	15	IP+		EST48827.1, 0.0
GL50803_6430*	14-3-3 protein	28,576	8	IP++		EST46224.1, 6E–115
GL50803_12795	Phosducin-like	26,919	6			EST41453.1, 1E–14
GL50803_9413	Protein disulfide isomerase PDI2	50,408	6	Precedents	57	EST43183.1, 5E–43
Trafficking						
GL50803_14373*	Dynamin	79,513	13	IP−	36	EST46023.1, 0.0
Unknown/*Giardia* specific						
GL50803_15264	Hypothetical protein	404,245	153			No
GL50803_39938	Hypothetical protein	716,474	95			EST41505.1, 4E–25
GL50803_17532	Hypothetical protein	66,334	57			EST45241.1, 3E–19
GL50803_15485	Hypothetical protein	751,987	55			EST41949.1, 9E–20
GL50803_13942	Hypothetical Protein	56,506	53			No
GL50803_7807	WD-40 repeat protein	59,785	51			EST44362.1, 2E–65
GL50803_17266	Ankyrin and WD repeat protein	14,462	47			No
GL50803_137711	Hypothetical protein	719,629	41			EST41949.1, 2E–49
GL50803_17596	Zinc finger domain protein	90,538	29			EST4938.1, 2E–09
GL50803_23897	Hypothetical protein	92,642	28			No
GL50803_99726	Hypothetical protein	11,183	25			No
GL50803_113592	Hypothetical protein	489,165	24			No
GL50803_5859	Hypothetical Protein	20,141	22			No
GL50803_20601	Hypothetical protein	11,136	22			No
GL50803_3559	Hypothetical protein	24,801	18			No
GL50803_14492	Hypothetical protein	54,020	15			No
GL50803_35487	Hypothetical protein	884,517	14			No
GL50803_8725	Hypothetical protein	51,753	11			No
GL50803_37350	Hypothetical protein	796,898	11			EST43354.1, 0.0
GL50803_35341	Hypothetical protein	776,894	11			EST45092.1, 1E–176
GL50803_15442	KIF binding domain	108,189	8			No
GL50803_137739	Hypothetical protein	211,474	8			No
GL50803_92602	Hypothetical protein	342,328	6			EST44629.1, 6E–73

[a] *, This protein was chosen for testing interaction with actin, as described in Results.
[b] +++, strong interactor; ++, moderate interactor; +, weak interactor; −, no interaction detected.
[c] The exponential values are BLAST Expect values, indicating the level of conservation between the homologs.

like kinase (S. Gourguechon and W. Z. Cande, unpublished data); because we did not find Polo in the actin data set, nor did we find actin in the Polo data set, we believe the low-abundance hits are likely false positives. The identity of these low-abundance hits may be useful for others using our same approach; therefore, we have identified the overlapping hits in Table S2 in the supplemental material.

Although once controversial, it is now clear that actin is part of the nucleoskeleton responsible for many nuclear processes, including transcriptional regulation, chromatin remodeling, and

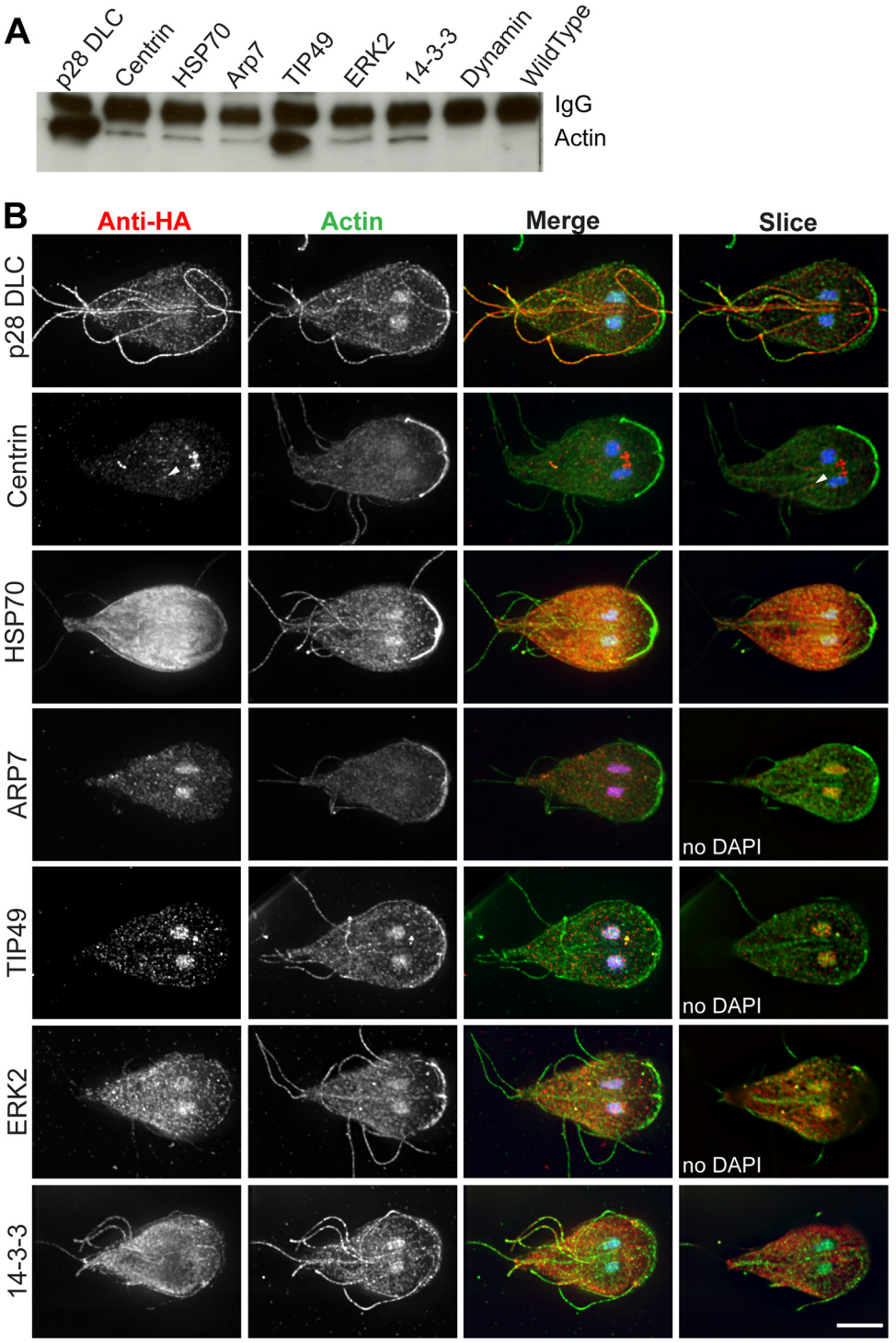

FIG 4 Validation of identified interacting proteins. (A) Immunoprecipitation from *Giardia* extracts of C-terminally HA-tagged interactors, followed by anti-actin Western blotting demonstrates that these proteins interact with actin. (B) Colocalization of actin and HA-tagged interacting proteins in *Giardia* trophozoites. Actin is green, HA tagged proteins are red, DNA is blue. The first three columns are maximal projections, and the last column is a single slice through the middle of the cell. Arrowhead marks centrin localization associated with the posterolateral flagella. Scale bar, 5 μm.

general maintenance of genome organization and integrity (reviewed in reference 38). In contrast to localization studies performed in model eukaryotes, where it is difficult to detect actin in the nucleus, giActin is readily detectable in the nuclei, suggesting that it has an important role in nuclear function (see Fig. 3B). Although we validated complex formation with actin for ARP7 and TIP49 (the second most abundant hit in terms of peptides/molecular weight), we identified six other proteins containing do-

mains that are consistent with a role in actin-based chromatin remodeling. It has been put forth that several proteins known to function in the cytoskeleton have roles in the nucleus; thus, they may have originally evolved to serve the genome (38). Our identification of conserved nuclear proteins and the lack of core cytoskeletal regulators are consistent with this notion.

Actin's role in the flagella is well established but largely ignored. Biochemical fractionation of flagella has shown that six of the seven inner dynein arm complexes are associated with actin (39). A conventional actin mutant of *Chlamydomonas*, ida5, lacks four of the inner-arm dynein complexes and, in this mutant, an actin-like protein, NAP, is upregulated to substitute for actin in the remaining two inner-arm dynein complexes, thus demonstrating the importance of actin to axonemal structure and function (39). Within the inner-arm dynein complexes, actin is thought to exist as a monomer in a complex with either a dimer of p28 or a monomer of centrin (32). Using super-resolution microscopy, we observed a regular repeating pattern for actin within all eight of the *Giardia* flagella (13). The precise molecular role of actin in the inner-arm dynein complexes remains enigmatic, but if actin simply acts as an adapter, it is perplexing to consider that *Giardia* may have lost proteins such as myosin, formin, and cofilin while maintaining actin's role in the flagella. Alternatively, some of the earliest functions of actin may include flagellar and nuclear processes.

Of the conserved proteins identified, 14-3-3 and ERK2 may be the most intriguing since they are likely regulators of actin dynamics or actin-related processes. 14-3-3 is known to play an important role in cytoskeletal regulation in other eukaryotes (40); however, the relationship between 14-3-3 and actin is complicated by multiple isoforms of 14-3-3 and conflicting results about 14-3-3 interactions with actin (reviewed in reference 41). In addition to our identification of 14-3-3 as an actin interactor, several efforts to define the 14-3-3 interactome in both *Giardia* and mammalian cells corroborate an actin–14-3-3 interaction (42–44). However, the current view is that 14-3-3 regulates actin through phospho-dependent interaction with the actin-depolymerizing protein cofilin and does not bind to actin directly (45, 46). Notably, *Giardia* lacks both cofilin and its regulatory kinase LIM. Perhaps a more direct regulation of actin by 14-3-3 underlies the well-characterized cofilin–14-3-3 interaction. Our analysis of 14-3-3's role in actin regulation is in preparation (J. Krtková, J. W. Xu, and A. R. Paredez, unpublished data).

Giardial ERK2 is a potential regulator of actin-related processes. *Giardia* contains two ERK homologs: a prototypical ERK, giERK1, and the ERK7-like protein giERK2 (47, 48). Although ERK stands for extracellular signal-regulated kinase, ERK7, unlike other mitogen-activated proteins, is atypical in that it is thought to be auto-activated rather than responding to external signals (49, 50). giERK2 lacks the extended C-terminal domain found in ERK7 and may not be regulated in the same manner, and yet *in vitro* kinase assays have shown that giERK2 is much more active than giERK1 (48). In other eukaryotes, ERK7 kinases have been shown to regulate protein secretion and cell proliferation (50, 51). Our identification of an actin-ERK2 complex in *Giardia* and the localization of this kinase in the nucleus and throughout the cell do not exclude potentially conserved function.

This initial characterization of actin-associated proteins in *Giardia* has focused on validating interaction with conserved proteins (see above), both because of the evolutionary implications and because these conserved proteins serve as proof of principle for our proteomic strategy. The largest group of identified proteins is, however, the novel/*Giardia*-specific category (see Table 1). We have begun to analyze the *Giardia*-specific interactors with the same endogenous-tagging approach used to study the conserved actin-interacting proteins. We have tagged 13 of the *Giardia*-specific proteins listed in Table 1 and have been able to immunoprecipitate giActin with 10 of these proteins (in preparation). Notably, five of these proteins localize to the nuclei, one localizes to the flagella, and the remaining proteins show a punctate pattern. None of the proteins identified thus far appear to colocalize with filamentous actin structures. Most canonical actin-binding proteins exclusively recognize globular or filamentous actin. The buffer conditions used in our affinity purification approach contained Ca^{2+} and ATP but lacked the Mg^{2+} and KCl typically found in buffers that support actin filament formation. Therefore, additional interactors remain to be discovered, and the set of interactors described here likely represents the globular giActin interactome. We did, however, test the ability of TS-Actin to polymerize, as assayed by ultracentrifugation (see Fig. S2 in the supplemental material). We observed that TS-Actin has some ability to pellet under filament-forming conditions that are consistent with the partial rescue we observed in our morpholino-knockdown experiments (Fig. 2). Future work will explore the identification of actin interactors in buffer conditions that support actin filament formation.

In this first exploration of the giActin interactome, we found both conserved and *Giardia*-specific interactors. The subset of canonical actin-binding proteins in *S. salmonicida* suggests loss of actin-binding proteins from *Giardia*. Therefore, the retention of actin-interacting proteins in the nucleus and flagella suggest these processes are the most constrained of any actin processes. In any case, the role of actin in the nucleoskeleton and flagella are likely some of actin's most ancient functions and remain relatively unexplored compared to the role of actin in the cytoskeleton. The set of novel/*Giardia*-specific proteins remain intriguing. Many of these proteins have no recognizable domains; therefore, elucidation of their function will be a challenge. Simultaneously, if functional experiments demonstrate these proteins to be essential, they will become potential therapeutic targets to treat giardiasis.

ACKNOWLEDGMENTS

We thank L. Kohlstaedt and the QB3 P/MSL for their assistance with the MudPIT analysis. We thank S. Gourguechon for technical assistance, for sharing his proteomic data, and for critical reading of the manuscript. We thank M. Steele-Ogus, W. Hardin, and J. J. Vicente for critical reading of the manuscript.

This research was sponsored by National Institutes of Health grant A1054693 to W.Z.C., National Science Foundation Postdoctoral Fellowship 0705351, and UW Biology Startup funds to A.R.P.

REFERENCES

1. **Cavalier-Smith T.** 2002. The phagotrophic origin of eukaryotes and phylogenetic classification of protozoa. Int. J. Syst. Evol. Microbiol. **52:**297–354. http://dx.doi.org/10.1099/ijs.0.02058-0.
2. **Ciccarelli FD, Doerks T, von Mering C, Creevey CJ, Snel B, Bork P.** 2006. Toward automatic reconstruction of a highly resolved tree of life. Science **311:**1283–1287. http://dx.doi.org/10.1126/science.1123061.
3. **Hampl V, Hug L, Leigh JW, Dacks JB, Lang BF, Simpson AG, Roger AJ.** 2009. Phylogenomic analyses support the monophyly of excavata and resolve relationships among eukaryotic "supergroups." Proc. Natl. Acad. Sci. U. S. A. **106:**3859–3864. http://dx.doi.org/10.1073/pnas.0807880106.

4. **Morrison HG, McArthur AG, Gillin FD, Aley SB, Adam RD, Olsen GJ, Best AA, Cande WZ, Chen F, Cipriano MJ, Davids BJ, Dawson SC, Elmendorf HG, Hehl AB, Holder ME, Huse SM, Kim UU, Lasek-Nesselquist E, Manning G, Nigam A, Nixon JE, Palm D, Passamaneck NE, Prabhu A, Reich CI, Reiner DS, Samuelson J, Svard SG, Sogin ML.** 2007. Genomic minimalism in the early diverging intestinal parasite *Giardia lamblia*. Science **317:**1921–1926. http://dx.doi.org/10.1126/science.1143837.
5. **Koonin E.** 2010. The origin and early evolution of eukaryotes in the light of phylogenomics. Genome Biol. **11:**209. http://dx.doi.org/10.1186/gb-2010-11-5-209.
6. **Keister DB.** 1983. Axenic culture of *Giardia lamblia* in Tyi-S-33 medium supplemented with bile. Trans. R. Soc. Trop. Med. Hyg. **77:**487–488. http://dx.doi.org/10.1016/0035-9203(83)90120-7.
7. **Gillin FD, Reiner DS, Gault MJ, Douglas H, Das S, Wunderlich A, Sauch JF.** 1987. Encystation and expression of cyst antigens by *Giardia lamblia* in vitro. Science **235:**1040–1043. http://dx.doi.org/10.1126/science.3547646.
8. **Sun CH, Tai JH.** 2000. Development of a tetracycline controlled gene expression system in the parasitic protozoan *Giardia lamblia*. Mol. Biochem. Parasitol. **105:**51–60. http://dx.doi.org/10.1016/S0166-6851(99)00163-2.
9. **Carpenter ML, Cande WZ.** 2009. Using morpholinos for gene knockdown in *Giardia intestinalis*. Eukaryot. Cell **8:**916–919. http://dx.doi.org/10.1128/EC.00041-09.
10. **Gourguechon S, Cande WZ.** 2011. Rapid tagging and integration of genes in *Giardia intestinalis*. Eukaryot. Cell **10:**142–145. http://dx.doi.org/10.1128/EC.00190-10.
11. **Dawson SC, Paredez AR.** 2013. Alternative cytoskeletal landscapes: cytoskeletal novelty and evolution in basal excavate protists. Curr. Opin. Cell Biol. **25:**134–141. http://dx.doi.org/10.1016/j.ceb.2012.11.005.
12. **Pollard TD.** 2003. The cytoskeleton, cellular motility, and the reductionist agenda. Nature **422:**741–745. http://dx.doi.org/10.1038/nature01598.
13. **Paredez AR, Assaf ZJ, Sept D, Timofejeva L, Dawson SC, Wang CJ, Cande WZ.** 2011. An actin cytoskeleton with evolutionarily conserved functions in the absence of canonical actin-binding proteins. Proc. Natl. Acad. Sci. U. S. A. **108:**6151–6156. http://dx.doi.org/10.1073/pnas.1018593108.
14. **Washburn MP, Wolters D, Yates JR, III.** 2001. Large-scale analysis of the yeast proteome by multidimensional protein identification technology. Nat. Biotechnol. **19:**242–247. http://dx.doi.org/10.1038/85686.
15. **Sagolla MS, Dawson SC, Mancuso JJ, Cande WZ.** 2006. Three-dimensional analysis of mitosis and cytokinesis in the binucleate parasite *Giardia intestinalis*. J. Cell Sci. **119:**4889–4900. http://dx.doi.org/10.1242/jcs.03276.
16. **Farthing MJG, Pereira MEA, Keusch GT.** 1982. *Giardia lamblia*: evaluation of roller bottle cultivation. Exp. Parasitol. **54:**410–415. http://dx.doi.org/10.1016/0014-4894(82)90050-9.
17. **Singer SM, Yee J, Nash TE.** 1998. Episomal and integrated maintenance of foreign DNA in *Giardia lamblia*. Mol. Biochem. Parasitol. **92:**59–69. http://dx.doi.org/10.1016/S0166-6851(97)00225-9.
18. **Eng JK, McCormack AL, Yates JR.** 1994. an approach to correlate tandem mass spectral data of peptides with amino acid sequences in a protein database. J. Am. Soc. Mass Spectrom. **5:**976–989. http://dx.doi.org/10.1016/1044-0305(94)80016-2.
19. **Tabb DL, McDonald WH, Yates JR, III.** 2002. DTASelect and Contrast: tools for assembling and comparing protein identifications from shotgun proteomics. J. Proteome Res. **1:**21–26. http://dx.doi.org/10.1021/pr015504q.
20. **Schneider CA, Rasband WS, Eliceiri KW.** 2012. NIH Image to ImageJ: 25 years of image analysis. Nat. Methods **9:**671–675. http://dx.doi.org/10.1038/nmeth.2089.
21. **Schmidt TG, Batz L, Bonet L, Carl U, Holzapfel G, Kiem K, Matulewicz K, Niermeier D, Schuchardt I, Stanar K.** 2013. Development of the Twin-Strep-Tag® and its application for purification of recombinant proteins from cell culture supernatants. Protein Expr. Purif. **92:**54–61. http://dx.doi.org/10.1016/j.pep.2013.08.021.
22. **Witte CP, Noel LD, Gielbert J, Parker JE, Romeis T.** 2004. Rapid one-step protein purification from plant material using the eight-amino acid StrepII epitope. Plant Mol. Biol. **55:**135–147. http://dx.doi.org/10.1007/s11103-004-0501-y.
23. **Junttila MR, Saarinen S, Schmidt T, Kast J, Westermarck J.** 2005. Single-step Strep-Tag purification for the isolation and identification of protein complexes from mammalian cells. Proteomics **5:**1199–1203. http://dx.doi.org/10.1002/pmic.200400991.
24. **Riedl J, Crevenna AH, Kessenbrock K, Yu JH, Neukirchen D, Bista M, Bradke F, Jenne D, Holak TA, Werb Z, Sixt M, Wedlich-Soldner R.** 2008. Lifeact: a versatile marker to visualize F-actin. Nat. Methods **5:**605–607. http://dx.doi.org/10.1038/nmeth.1220.
25. **Adam RD.** 2001. Biology of *Giardia lamblia*. Clin. Microbiol. Rev. **14:**447–475. http://dx.doi.org/10.1128/CMR.14.3.447-475.2001.
26. **Hansen WR, Tulyathan O, Dawson SC, Cande WZ, Fletcher DA.** 2006. *Giardia lamblia* attachment force is insensitive to surface treatments. Eukaryot. Cell **5:**781–783. http://dx.doi.org/10.1128/EC.5.4.781-783.2006.
27. **Benchimol M.** 2004. Mitosis in *Giardia lamblia*: multiple modes of cytokinesis. Protist **155:**33–44. http://dx.doi.org/10.1078/1434461000162.
28. **Tumova P, Kulda J, Nohynkova E.** 2007. Cell division of *Giardia intestinalis*: assembly and disassembly of the adhesive disc, and the cytokinesis. Cell Motil. Cytoskel. **64:**288–298. http://dx.doi.org/10.1002/cm.20183.
29. **Sternlicht H, Farr GW, Sternlicht ML, Driscoll JK, Willison K, Yaffe MB.** 1993. The T-complex polypeptide-1 complex is a chaperonin for tubulin and actin in vivo. Proc. Natl. Acad. Sci. U. S. A. **90:**9422–9426. http://dx.doi.org/10.1073/pnas.90.20.9422.
30. **Bui KH, Sakakibara H, Movassagh T, Oiwa K, Ishikawa T.** 2008. Molecular architecture of inner dynein arms in situ in *Chlamydomonas reinhardtii* flagella. J. Cell Biol. **183:**923–932. http://dx.doi.org/10.1083/jcb.200808050.
31. **Piperno G, Luck DJL.** 1979. Actin-like protein is a component of axonemes from *Chlamydomonas* flagella. J. Biol. Chem. **254:**2187–2190.
32. **Yanagisawa H, Kamiya R.** 2001. Association between actin and light chains in *Chlamydomonas* flagellar inner-arm dyneins. Biochem. Biophys. Res. Commun. **288:**443–447. http://dx.doi.org/10.1006/bbrc.2001.5776.
33. **Xu F, Jerlstrom-Hultqvist J, Einarsson E, Astvaldsson A, Svard SG, Andersson JO.** 2014. The genome of spironucleus salmonicida highlights a fish pathogen adapted to fluctuating environments. PLoS Genet. **10:**e1004053. http://dx.doi.org/10.1371/journal.pgen.1004053.
34. **Carlton JM, Hirt RP, Silva JC, Delcher AL, Schatz M, Zhao Q, Wortman JR, Bidwell SL, Alsmark UC, Besteiro S, Sicheritz-Ponten T, Noel CJ, Dacks JB, Foster PG, Simillion C, Van de Peer Y, Miranda-Saavedra D, Barton GJ, Westrop GD, Muller S, Dessi D, Fiori PL, Ren Q, Paulsen I, Zhang H, Bastida-Corcuera FD, Simoes-Barbosa A, Brown MT, Hayes RD, Mukherjee M, Okumura CY, Schneider R, Smith AJ, Vanacova S, Villalvazo M, Haas BJ, Pertea M, Feldblyum TV, Utterback TR, Shu CL, Osoegawa K, de Jong PJ, Hrdy I, Horvathova L, Zubacova Z, Dolezal P, Malik SB, Logsdon JM, Jr, Henze K, Gupta A, Wang CC, Dunne RL, Upcroft JA, Upcroft P, White O, Salzberg SL, Tang P, Chiu CH, Lee YS, Embley TM, Coombs GH, Mottram JC, Tachezy J, Fraser-Liggett CM, Johnson PJ.** 2007. Draft genome sequence of the sexually transmitted pathogen *Trichomonas vaginalis*. Science **315:**207–212. http://dx.doi.org/10.1126/science.1132894.
35. **Nagata K, Takagi K, Hashida T, Ichikawa Y.** 1985. A monovalent cation-sensitive actin-binding factor in a myeloid leukemia cell line. Cell Struct. Funct **10:**105–120. http://dx.doi.org/10.1247/csf.10.105.
36. **Yamada H, Abe T, Satoh A, Okazaki N, Tago S, Kobayashi K, Yoshida Y, Oda Y, Watanabe M, Tomizawa K, Matsui H, Takei K.** 2013. Stabilization of actin bundles by a dynamin 1/cortactin ring complex is necessary for growth cone filopodia. J. Neurosci. **33:**4514–4526. http://dx.doi.org/10.1523/jneurosci.2762-12.2013.
37. **Jerlstrom-Hultqvist J, Stadelmann B, Birkestedt S, Hellman U, Svard SG.** 2012. Plasmid vectors for proteomic analyses in *Giardia*: purification of virulence factors and analysis of the proteasome. Eukaryot. Cell **11:**864–873. http://dx.doi.org/10.1128/ec.00092-12.
38. **Simon DN, Wilson KL.** 2011. The nucleoskeleton as a genome-associated dynamic "network of networks." Nat. Rev. Mol. Cell Biol. **12:**695–708. http://dx.doi.org/10.1038/nrm3207.
39. **KatoMinoura T, Hirono M, Kamiya R.** 1997. *Chlamydomonas* inner-arm dynein mutant, Ida5, has a mutation in an actin-encoding gene. J. Cell Biol. **137:**649–656. http://dx.doi.org/10.1083/jcb.137.3.649.
40. **Roth D, Birkenfeld J, Betz H.** 1999. Dominant-negative alleles of 14-3-3 proteins cause defects in actin organization and vesicle targeting in the yeast *Saccharomyces cerevisiae*. FEBS Lett. **460:**411–416. http://dx.doi.org/10.1016/S0014-5793(99)01383-6.
41. **Sluchanko NN, Gusev NB.** 2010. 14-3-3 proteins and regulation of cytoskeleton. Biochemistry (Mosc.) **75:**1528–1546.
42. **Lalle M, Camerini S, Cecchetti S, Sayadi A, Crescenzi M, Pozio E.** 2012. Interaction network of the 14-3-3 protein in the ancient protozoan parasite *Giardia duodenalis*. J. Proteome Res. **11:**2666–2683. http://dx.doi.org/10.1021/pr3000199.
43. **Liang S, Yu Y, Yang P, Gu S, Xue Y, Chen X.** 2009. Analysis of the

protein complex associated with 14-3-3 epsilon by a deuterated-leucine labeling quantitative proteomics strategy. J. Chromatogr. B Anal. Technol. Biomed. Life Sci. **877:**627–634. http://dx.doi.org/10.1016/j.jchromb.2009.01.023.

44. **Pozuelo Rubio M, Geraghty KM, Wong BH, Wood NT, Campbell DG, Morrice N, Mackintosh C.** 2004. 14-3-3 affinity purification of over 200 human phosphoproteins reveals new links to regulation of cellular metabolism, proliferation, and trafficking. Biochem. J. **379:**395–408. http://dx.doi.org/10.1042/BJ20031797.
45. **Birkenfeld J, Betz H, Roth D.** 2003. Identification of cofilin and Lim-domain-containing protein kinase 1 as novel interaction partners of 14-3-3 zeta. Biochem. J. **369:**45–54. http://dx.doi.org/10.1042/BJ20021152.
46. **Gohla A, Bokoch GM.** 2002. 14-3-3 regulates actin dynamics by stabilizing phosphorylated cofilin. Curr. Biol. **12:**1704–1710. http://dx.doi.org/10.1016/S0960-9822(02)01184-3.
47. **Manning G, Reiner DS, Lauwaet T, Dacre M, Smith A, Zhai Y, Svard S, Gillin FD.** 2011. The minimal kinome of *Giardia lamblia* illuminates early kinase evolution and unique parasite biology. Genome Biol. **12:**R66. http://dx.doi.org/10.1186/gb-2011-12-7-r66.
48. **Ellis JG, Davila M, Chakrabarti R.** 2003. Potential involvement of extracellular signal-regulated kinase 1 and 2 in encystation of a primitive eukaryote, *Giardia lamblia*: stage-specific activation and intracellular localization. J. Biol. Chem. **278:**1936–1945. http://dx.doi.org/10.1074/jbc.M209274200.
49. **Abe MK, Kahle KT, Saelzler MP, Orth K, Dixon JE, Rosner MR.** 2001. Erk7 is an autoactivated member of the MAPK family. J. Biol. Chem. **276:**21272–21279. http://dx.doi.org/10.1074/jbc.M100026200.
50. **Abe MK, Kuo WL, Hershenson MB, Rosner MR.** 1999. Extracellular signal-regulated kinase 7 (Erk7), a novel Erk with a C-terminal domain that regulates its activity, its cellular localization, and cell growth. Mol. Cell. Biol. **19:**1301–1312.
51. **Zacharogianni M, Kondylis V, Tang Y, Farhan H, Xanthakis D, Fuchs F, Boutros M, Rabouille C.** 2011. Erk7 is a negative regulator of protein secretion in response to amino acid starvation by modulating Sec16 membrane association. EMBO J. **30:**3684–3700. http://dx.doi.org/10.1038/emboj.2011.253.
52. **Turturici G, Geraci F, Candela ME, Giudice G, Gonzalez F, Sconzo G.** 2008. Hsp70 localizes differently from chaperone Hsc70 in mouse mesoangioblasts under physiological growth conditions. J. Mol. Histol. **39:**571–578. http://dx.doi.org/10.1007/s10735-008-9197-7.
53. **Zhao Z, Liu H, Wang X, Li Z.** 2011. Separation and identification of HSP-associated protein complexes from pancreatic cancer cell lines using 2D CN/SDS-PAGE coupled with mass spectrometry. J. Biomed. Biotechnol. **2011:**193052. http://dx.doi.org/10.1155/2011/193052.
54. **Rando OJ, Zhao KJ, Janmey P, Crabtree GR.** 2002. Phosphatidylinositol-dependent actin filament binding by the Swi/Snf-like Baf chromatin remodeling complex. Proc. Natl. Acad. Sci. U. S. A. **99:**2824–2829. http://dx.doi.org/10.1073/pnas.032662899.
55. **Park J, Wood MA, Cole MD.** 2002. Baf53 forms distinct nuclear complexes and functions as a critical c-myc-interacting nuclear cofactor for oncogenic transformation. Mol. Cell. Biol. **22:**1307–1316. http://dx.doi.org/10.1128/MCB.22.5.1307-1316.2002.
56. **Choi J, Heo K, An WJ.** 2009. Cooperative action of Tip48 and Tip49 in H2a.Z exchange catalyzed by acetylation of nucleosomal H2a. Nucleic Acids Res. **37:**5993–6007. http://dx.doi.org/10.1093/nar/gkp660.
57. **Safran M, Farwell AP, Leonard JL.** 1992. Thyroid hormone-dependent redistribution of the 55-kilodalton monomer of protein disulfide isomerase in cultured glial cells. Endocrinology **131:**2413–2418. http://dx.doi.org/10.1210/endo.131.5.1425439.